Frascati Physics Series Vol. XXXV (2004), pp. 367-376
HEAVY QUARKS AND LEPTONS - San Juan, Puerto Rico, June 1-5, 2004

LATEST RESULTS FROM NA48 ON K_L & K_S CP VIOLATING RELATED RARE DECAYS

Mayda M. Velasco
Northwestern University
Department of Physics & Astronomy,
2145 Sheridan Rd, Evanston IL 60208, USA

ABSTRACT

We present the results of a search for $K_S \to \pi^0 e^+ e^-$ and $K_S \to \pi^0 \mu^+ \mu^-$, from the NA48 high intensity 2002 K_S run. These channels are needed to fully understand their CP-violating contributions in the corresponding K_L decays. In addition, we show the collected data sample of $K^\pm \to \pi^\pm e^+ e^-$ and $K^\pm \to \pi^\pm \mu^+ \mu^-$ from the 2003 $K^\pm$ run. That data sample will help determine whether the resulting interference between the direct and indirect CP–violating amplitudes in $K_L \to \pi^0 \ell^+ \ell^-$ are constructive or destructive.

1 Introduction

Physics beyond the standard model could be accessed from $K \to \pi\ell\ell$ from existing machines! New physics could manifest itself through loops for K_L, K_S, and $K^\pm$ in these channels. In this talk, we focus on recent NA48 results

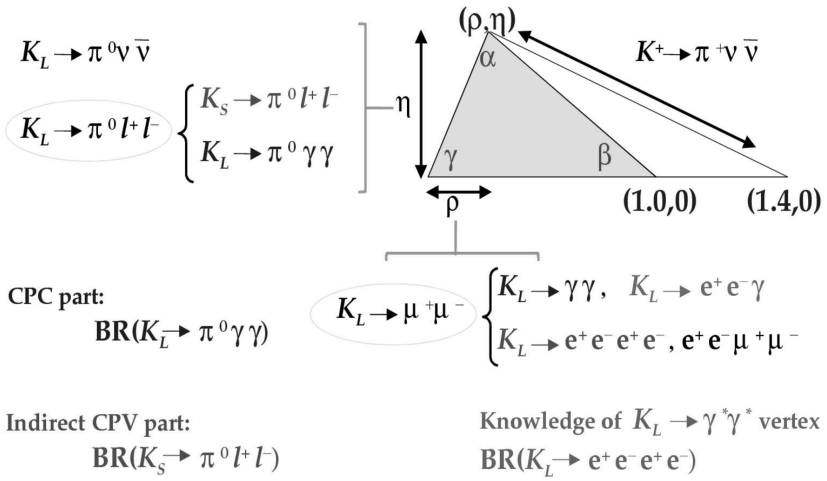

Figure 1: *Unitary triangle in the Kaon system, and contribution from various rare decays.*

on K_L, K_S, and $K^\pm$ rare decays that will allow us to predict the CP conserving(CPC), CP-violating(CPV) and interference components of $K_L \to \pi\ell\ell$, where $\ell = e, \mu$. These processes will allow us to perform high-precision tests of Standard Model (SM) flavor physics, including the CKM mechanism for CP violation (Fig. 1), and define very sensitive probes of new physics.

The CKM matrix has the explicit form

$$V = \begin{pmatrix} V_{ud} & V_{us} & V_{ub} \\ V_{cd} & V_{cs} & V_{cb} \\ V_{td} & V_{ts} & V_{tb} \end{pmatrix} \simeq \tag{1}$$

$$\begin{pmatrix} 1-\lambda^2/2 & \lambda & A\lambda^3(\varrho - i\eta) \\ -\lambda & 1-\lambda^2/2 & A\lambda^2 \\ A\lambda^3(1-\varrho-i\eta) & -A\lambda^2 & 1 \end{pmatrix} \tag{2}$$

where the second expression is the useful approximate representation due to Wolfenstein with the parameters λ, A, ϱ and the complex phase η. The absolute values of the elements of the CKM matrix show a hierarchical pattern with the diagonal elements being close to unity, the elements $|V_{us}| = \lambda$ and $|V_{cd}|$ being of order 0.2, the elements $|V_{cb}| = A\lambda^2$ and $|V_{ts}|$ of order $4 \cdot 10^{-2}$ whereas $|V_{ub}|$ and

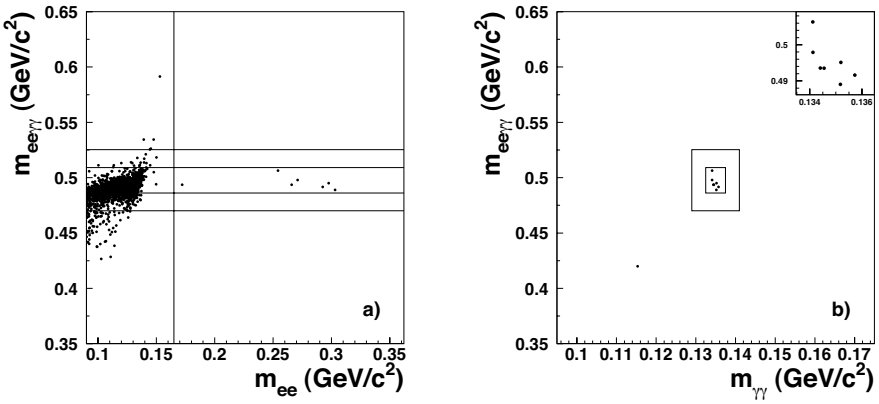

Figure 2: *Scatter plot of $m_{ee\gamma\gamma}$ versus m_{ee} (a) and $m_{ee\gamma\gamma}$ versus $m_{\gamma\gamma}$ (b) for events passing all the cuts described in Ref.* [1]. *The regions of 3σ and 6σ are shown.*

$|V_{td}|$ are of order $5{\cdot}10^{-3}$. Recent results on λ based on kaon semileptonic decays were discussed at this conference, but in this talk we will focus on channels that provide the ϱ and η parameters like $K_L \to \pi^0 e^+ e^-$ and $K_L \to \pi^0 \mu^+ \mu^-$. As shown in Fig. 1, this requires the measurement of several rare kaon decays, like $K_S \to \pi^0 \ell^+ \ell^-$ to determine the indirect CPV component and the interference term, $K_L \to \pi^0 \gamma\gamma$ to determine the CPC component, and $K^\pm \to \pi^\pm \ell^+ \ell^-$ as extra information to determine the sign of the interference term.

2 Results and Discussion for the $K_S \to \pi^0 \ell^+ \ell^- (\ell = e, \mu)$

The K_S run used in these analyses took place in 2002 and it had a total of $(2-4) \times 10^{10}$ K_S decays. As shown in Fig. 2, seven events were found in the $K_S \to \pi^0 e^+ e^-$ signal region, with a background estimate of $0.15^{+0.10}_{-0.04}$ events (Fig. 3), while six events were found in the signal region for $K_S \to \pi^0 \mu^+ \mu^-$ (Fig. 4), with a background estimate of $0.22^{+0.18}_{-0.11}$ events (Fig. 5). These are the first observations for $K_S \to \pi^0 e^+ e^-$ and $K_S \to \pi^0 \mu^+ \mu^-$ decays.

The kinematic properties of the $K_S \to \pi^0 e^+ e^-$ and $K_S \to \pi^0 \mu^+ \mu^-$ candidates were consistent with those expected based on Monte Carlo simulation of the signal.

Taking into account the trigger efficiency, the acceptance and the flux,

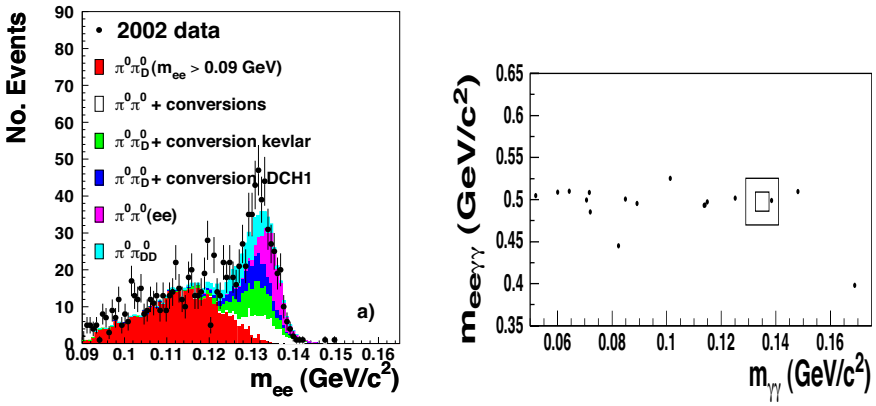

Figure 3: *(a) Distributions of m_{ee} after all the cuts have been applied. Superimposed we show the Monte Carlo predictions from all important sources. Figure (a) shows the components with opposite-sign tracks. (b)Scatter plot of $m_{ee\gamma\gamma}$ versus $m_{\gamma\gamma}$ for events selected as $K_L \to e^+e^-\gamma\gamma$ in the 2001 data used to estimate the background. The boxes represent the 3σ and 6σ regions.*

the $K_S \to \pi^0 e^+ e^-$ branching ratio was measured to be [1]:

$$B(K_S \to \pi^0 e^+ e^-) = [5.8^{+2.8}_{-2.3}(stat) \pm 0.8(syst)] \times 10^{-9}, \quad (3)$$

and the $K_S \to \pi^0 \mu^+ \mu^-$ [2]:

$$B(K_S \to \pi^0 \mu^+ \mu^-) = [2.9^{+1.5}_{-1.2}(stat) \pm 0.2(syst)] \times 10^{-9}. \quad (4)$$

The results for $K_S \to \pi^0 e^+ e^-$ includes the extrapolation to the low $m_{e^+e^-}$-region excluded from the analysis in order to avoid backgrounds. These results are consistent within errors with the recent predictions based on Chiral Perturbation Theory [4, 5].

2.1 Test of Chiral Perturbation Theory

Chiral Perturbation Theory (ChPT) can be used to predict the branching ratio for $K_S \to \pi^0 \ell^+ \ell^-$ and the corresponding dilepton mass spectrum, $m_{\ell\ell}$. The measurement presented here tests these predictions and constrains the parameters of the model.

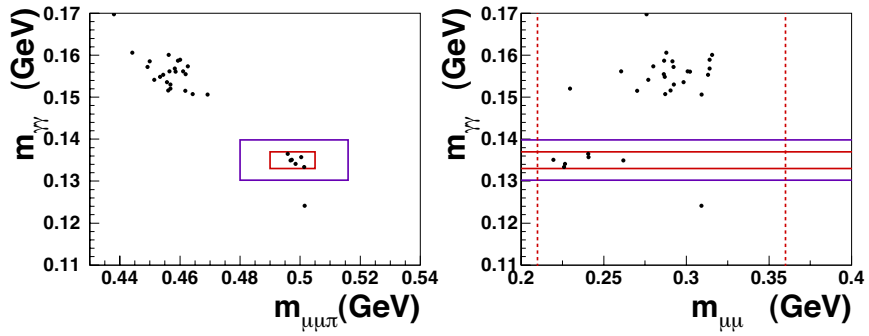

Figure 4: *Scatter plot for the events passing all the cuts described in* [2]*: (a) for the $m_{\gamma\gamma}$ versus $m_{\mu\mu\pi}$ plane and (b) for the $m_{\gamma\gamma}$ versus $m_{\mu\mu}$ plane. The 2.5σ and the 6σ signal and control regions and the $m_{\mu\mu}$ kinematic limits are also shown.*

The $K_S \to \pi^0\ell^+\ell^-$ branching ratios can be expressed as a function of two parameters, a_S and b_S [4]:

$$B(K_S \to \pi^0 e^+ e^-) = \left[0.01 - 0.76a_S - 0.21b_S + 46.5a_S^2 + 12.9a_S b_S + 1.44b_S^2\right] \times 10^{-10} \quad (5)$$

$$B(K_S \to \pi^0 \mu^+ \mu^-) = \left[0.07 - 4.52a_S - 1.50b_S + 98.7a_S^2 + 57.7a_S b_S + 8.95b_S^2\right] \times 10^{-11} \quad (6)$$

where the total form factor is $W_S(z) = G_F m_K^2(a_S + b_S z) + W_S^{\pi\pi}(z)$, $z = m_{\ell\ell}^2/m_K^2$, m_K is the kaon mass, $m_{\ell\ell}$ is the invariant mass of the two leptons, and $W_S^{\pi\pi}(z)$ is expected to be small. Assuming VMD, which predicts $b_S = 0.4\,a_S$ [4], the value of the parameter $|a_S|$ can be obtained from the measurement of the individual $K_S \to \pi^0\ell^+\ell^-$ branching ratios via the relations [6]

$$B(K_S \to \pi^0 e^+ e^-) \simeq 5.2 \times 10^{-9}\, a_S^2, \quad (7)$$

$$B(K_S \to \pi^0 \mu^+ \mu^-) \simeq 1.2 \times 10^{-9}\, a_S^2. \quad (8)$$

Using our new results for these branching ratios, the value of the parameter $|a_S|$ is found to be:

$$|a_S|_{ee} = 1.06^{+0.26}_{-0.21} \pm 0.07,$$

$$|a_S|_{\mu\mu} = 1.54^{+0.40}_{-0.32} \pm 0.06.$$

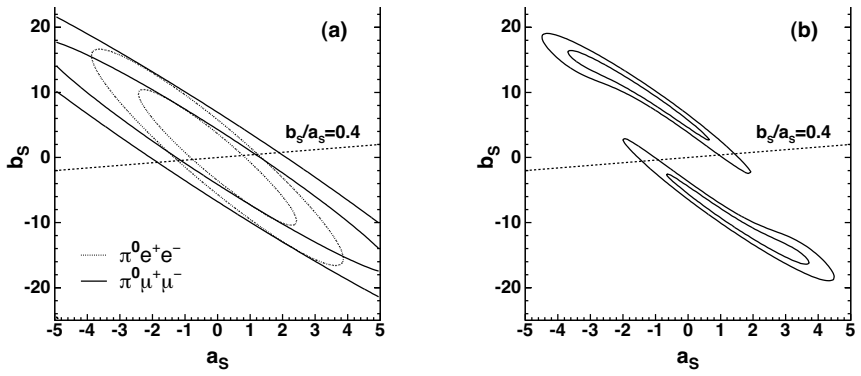

Figure 6: *(a) Allowed regions of a_S and b_S determined from the observed number of $K_S \to \pi^0\mu^+\mu^-$ and $K_S \to \pi^0e^+e^-$ events separately. The region between the inner and outer solid (dashed) elliptical contours is the allowed region for $K_S \to \pi^0\mu^+\mu^-$ ($K_S \to \pi^0e^+e^-$) at 68% CL. (b) Allowed regions of a_S and b_S for the $K_S \to \pi^0\mu^+\mu^-$ and $K_S \to \pi^0e^+e^-$ channels combined. The inner (outer) contour of each pair delimits the 1σ (2σ) allowed region from the combined log-likelihood. The dashed straight line in both plots corresponds to $b_S = 0.4a_S$, as predicted by the VMD model.*

assessment of the linear dependence of the form factor on z.

2.2 CPV component of $K_L \to \pi^0\ell^+\ell^-$

The branching ratios for the decay $K_S \to \pi^0\ell^+\ell^-$ ($\ell = e, \mu$) measured by NA48 allows us to predict the CPV contribution to the branching ratio of the corresponding K_L decay, $K_L \to \pi^0\ell^+\ell^-$, as a function of $\mathrm{Im}(\lambda_t)$ to within a sign ambiguity [8]:

$$B(K_L \to \pi^0\ell^+\ell^-)_{\mathrm{CPV}} \times 10^{12} = C_{\mathrm{MIX}} \pm C_{\mathrm{INT}} \left(\frac{\mathrm{Im}(\lambda_t)}{10^{-4}}\right) + C_{\mathrm{DIR}} \left(\frac{\mathrm{Im}(\lambda_t)}{10^{-4}}\right)^2 , \quad (11)$$

where

$$\begin{aligned}
C^{ee}_{\mathrm{MIX}} &= 3.0 \times 10^9\, B(K_S \to \pi^0e^+e^-), & C^{\mu\mu}_{\mathrm{MIX}} &= 3.1 \times 10^9\, B(K_S \to \pi^0\mu^+\mu^-),\\
C^{ee}_{\mathrm{INT}} &= 8.6 \times 10^4 \sqrt{B(K_S \to \pi^0e^+e^-)}, & C^{\mu\mu}_{\mathrm{INT}} &= 4.6 \times 10^4 \sqrt{B(K_S \to \pi^0\mu^+\mu^-)},\\
C^{ee}_{\mathrm{DIR}} &= 2.4 & C^{\mu\mu}_{\mathrm{DIR}} &= 1.0.
\end{aligned}$$

C_{INT} is the coefficient for the term due to the interference between the direct (C_{DIR}) and indirect (C_{MIX}) CPV components, and $\lambda_t = V_{td}V^*_{ts}$.

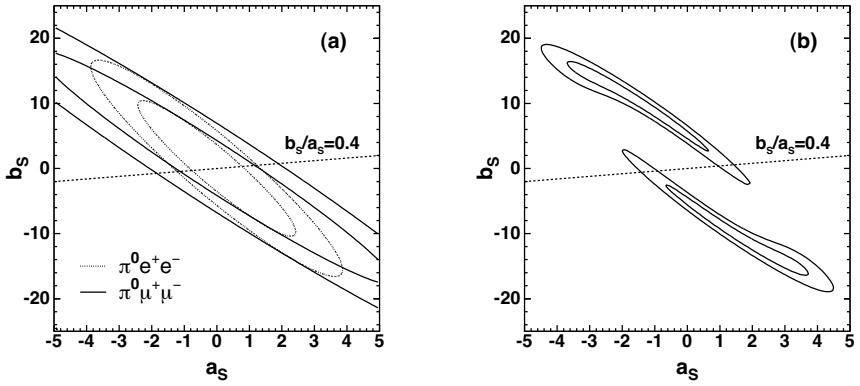

Figure 6: *(a) Allowed regions of a_S and b_S determined from the observed number of $K_S \to \pi^0\mu^+\mu^-$ and $K_S \to \pi^0e^+e^-$ events separately. The region between the inner and outer solid (dashed) elliptical contours is the allowed region for $K_S \to \pi^0\mu^+\mu^-$ ($K_S \to \pi^0e^+e^-$) at 68% CL. (b) Allowed regions of a_S and b_S for the $K_S \to \pi^0\mu^+\mu^-$ and $K_S \to \pi^0e^+e^-$ channels combined. The inner (outer) contour of each pair delimits the 1σ (2σ) allowed region from the combined log-likelihood. The dashed straight line in both plots corresponds to $b_S = 0.4a_S$, as predicted by the VMD model.*

assessment of the linear dependence of the form factor on z.

2.2 CPV component of $K_L \to \pi^0\ell^+\ell^-$

The branching ratios for the decay $K_S \to \pi^0\ell^+\ell^-$ ($\ell = e, \mu$) measured by NA48 allows us to predict the CPV contribution to the branching ratio of the corresponding K_L decay, $K_L \to \pi^0\ell^+\ell^-$, as a function of $\mathrm{Im}(\lambda_t)$ to within a sign ambiguity [8]:

$$B(K_L \to \pi^0\ell^+\ell^-)_{\mathrm{CPV}} \times 10^{12} = C_{\mathrm{MIX}} \pm C_{\mathrm{INT}} \left(\frac{\mathrm{Im}(\lambda_t)}{10^{-4}}\right) + C_{\mathrm{DIR}} \left(\frac{\mathrm{Im}(\lambda_t)}{10^{-4}}\right)^2 , \qquad (11)$$

where

$$\begin{aligned} C^{ee}_{\mathrm{MIX}} &= 3.0 \times 10^9\, B(K_S \to \pi^0e^+e^-), & C^{\mu\mu}_{\mathrm{MIX}} &= 3.1 \times 10^9\, B(K_S \to \pi^0\mu^+\mu^-), \\ C^{ee}_{\mathrm{INT}} &= 8.6 \times 10^4 \sqrt{B(K_S \to \pi^0e^+e^-)}, & C^{\mu\mu}_{\mathrm{INT}} &= 4.6 \times 10^4 \sqrt{B(K_S \to \pi^0\mu^+\mu^-)}, \\ C^{ee}_{\mathrm{DIR}} &= 2.4 & C^{\mu\mu}_{\mathrm{DIR}} &= 1.0. \end{aligned}$$

C_{INT} is the coefficient for the term due to the interference between the direct (C_{DIR}) and indirect (C_{MIX}) CPV components, and $\lambda_t = V_{td}V^*_{ts}$.

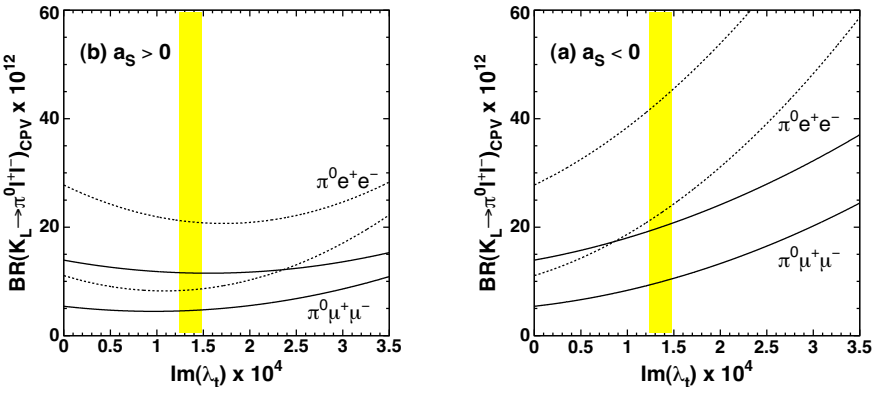

Figure 7: *Predicted CPV component of the* $K_L \to \pi^0\mu^+\mu^-$ *(solid curves) and* $K_L \to \pi^0 e^+ e^-$ *(dashed curves) branching ratios as a function of* $\mathrm{Im}(\lambda_t)$ *assuming (a)* $a_S < 0$ *and (b)* $a_S > 0$*. Each pair of curves delimits the allowed range derived from the* $\pm 1\sigma$ *measured values of* $|a_S|$*. The vertical shaded band corresponds to the world average value of* $\mathrm{Im}(\lambda_t)$*.*

Taking the central value of the measured branching ratio $B(K_S \to \pi^0\ell^+\ell^-)$ and $\mathrm{Im}(\lambda_t) = 1.36 \times 10^{-4}$ [9] gives:

$$B(K_L \to \pi^0 e^+ e^-)_{CPV} \times 10^{12} \approx 17.2_{\text{mixing}} \pm 9.4_{\text{interference}} + 4.7_{\text{direct}}; \quad (12)$$

$$B(K_L \to \pi^0 \mu^+ \mu^-)_{CPV} \times 10^{12} \approx 8.8_{\text{mixing}} \pm 3.3_{\text{interference}} + 1.8_{\text{direct}}. \quad (13)$$

The predicted dependence of $B(K_L \to \pi^0\ell^+\ell^-)_{\mathrm{CPV}}$ on $\mathrm{Im}(\lambda_t)$ is shown in Fig. 7 assuming VMD.

2.3 SM prediction for $K_L \to \pi^0\ell^+\ell^-$

The CPC component of $K_L \to \pi^0\ell^+\ell^-$ decays can be constrained using NA48 and KTeV measurements of the decay $K_L \to \pi^0\gamma\gamma$ [10, 11]. A recent analysis based on ChPT obtained the prediction $(5.2 \pm 1.6) \times 10^{-12}$ [8] for the muon channel, while it is negligible for the electron.

Combining the CPV and the CPC components, the central value for the total $K_L \to \pi^0 e^+ e^- (K_L \to \pi^0\mu^+\mu^-)$ branching ratio is estimated to be $32(19) \times 10^{-12}$ or $13(12) \times 10^{-12}$, depending on the sign of the interference term between the direct and the indirect (mixing) amplitudes. This estimate is consistent with the present experimental upper limit presented by KTeV

in this conference, that is $B(K_L \to \pi^0 e^+ e^-)$ of 2.8×10^{-10}(90% CL) and $B(K_L \to \pi^0 \mu^+ \mu^-)$ of 3.8×10^{-10}(90% CL).

3 Results and Discussion for the $K^\pm \to \pi^\pm \ell^+ \ell^-$

In principle, χPT theory can predict whether the resulting interference between the direct and indirect CP–violating amplitudes in $K_L \to \pi^0 \ell^+ \ell^-$ are constructive or destructive. To gain confidence in this model, we must compare its predictions for the decay rate and the invariant $\ell^+ \ell^-$ mass spectrum. There are not enough events in the NA48 $K_S \to \pi^0 e^+ e^-$ and $K_S \to \pi^0 \mu^+ \mu^-$ data sample. Therefore, analyses of mass spectrum for $K^\pm \to \pi^\pm e^+ e^-$ and $K^\pm \to \pi^\pm \mu^+ \mu^-$ will be studied instead.

After combining the data from the 2003 and 2004 $K^\pm$ run, we will have a $K^\pm \to \pi^\pm e^+ e^-$ that will be as large as the world data sample, that is, we will have more than 10,000 events. The current world data on $K^\pm \to \pi^\pm \mu^+ \mu^-$ consist of only 800 events. The NA48 sample will be at least three times larger. In both channels the background levels will be low, see Fig. 8.

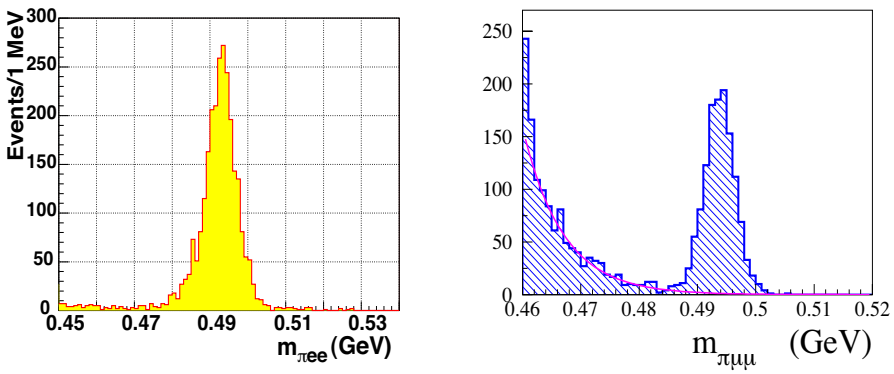

Figure 8: *NA48 reconstructed $K^\pm \to \pi^\pm e^+ e^-$ and $K^\pm \to \pi^\pm \mu^+ \mu^-$ events for a fraction of the available data sample.*

References

1. J.R. Batley *et al.*, Physics Letters B576 (2003) 43.

2. J.R. Batley *et al.*, CERN-PH-EP Preprint 2004-025, Accepted for publication by Physics Letters.

3. J.R. Batley *et al.*, Physics Letters B544 (2002) 97.

4. G. D'Ambrosio, G. Ecker, G. Isidori and J. Portoles, Journal of High Energy Physics 08 (1998) 004.

5. S. Friot, D. Greynat, and E. de Rafael, "Rare Kaon Decays Revisited," hep-ph/0404136.

6. G. Buchalla, G. D'Ambrosio and G. Isidori, Nuclear Physics B672 (2003) 387.

7. G. Ecker, A. Pich, and E. de Rafael, Nuclear Physics B291 (1987) 692.

8. G. Isidori, C. Smith and R. Unterdorfer, "The rare decay $K_L \to \pi^0 \mu\mu$ within the SM," hep-ph/0404127.

9. M. Battaglia *et al.*, "The CKM matrix and the unitarity triangle," hep-ph/0304132.

10. A. Lai *et al.*, Physics Letters B536 (2002) 229.

11. A. Alavi-Harati *et al.*, Physical Review Letters 83 (1999) 917.